Ke *et al. Soft Sci* 2023;3:21
DOI: 10.20517/ss.2023.14

Soft Science

Research Article

Open Access

Check for updates

Reduced graphene oxide reinforced PDA-Gly-PVA composite hydrogel as strain sensors for monitoring human motion

Xiaoling Ke[1], Xiaojiang Mu[1], Siyi Chen[2], Zhixiang Zhang[1], Jianhua Zhou[1,*], Yulian Chen[1], Jie Gao[1], Jing Liu[1], Xiaoyang Wang[1,3], Chuanguo Ma[1], Lei Miao[1,*]

[1]Guangxi Key Laboratory of Information Materials, Engineering Research Center of Electronic Information Materials and Devices, Ministry of Education, School of Materials Science and Engineering, Guilin University of Electronic Technology, Guilin 541004, Guangxi, China.
[2]College of Arts and Science, University of Tokyo, Tokyo 1538902, Japan.
[3]Department of Chemical Systems Engineering, Graduate School of Engineering, Nagoya University, Nagoya 464-8603, Japan.

[*]**Correspondence to:** Prof. Jianhua Zhou, Prof. Lei Miao, Guangxi Key Laboratory of Information Materials, Engineering Research Center of Electronic Information Materials and Devices, Ministry of Education, School of Materials Science and Engineering, Guilin University of Electronic Technology, No.1 Jinji Road, Qixing District, Guilin 541004, Guangxi, China. E-mail: jianhuazhou@guet.edu.cn; miaolei@guet.edu.cn

[*]**How to cite this article:** Ke X, Mu X, Chen S, Zhang Z, Zhou J, Chen Y, Gao J, Liu J, Wang X, Ma C, Miao L. Reduced graphene oxide reinforced PDA-Gly-PVA composite hydrogel as strain sensors for monitoring human motion. *Soft Sci* 2023;3:21. https://dx.doi.org/10.20517/ss.2023.14

Received: 21 Mar 2023 **First Decision:** 20 Apr 2023 **Revised:** 11 May 2023 **Accepted:** 23 May 2023 **Published:** 3 Jul 2023

Academic Editor: Zhifeng Ren **Copy Editor:** Lin He **Production Editor:** Lin He

Abstract

Hydrogels with soft, skin-friendly properties and high biocompatibility are promising alternatives to traditional sensors. However, balancing electrical conductivity and sensitivity remains a significant challenge. The sensitivity-improved strain sensor was designed by reduced graphene oxide (rGO) reinforced polydopamine (PDA)-glycerol (Gly)-polyvinyl alcohol composite hydrogels (PGPHs). The hydrogels exhibited excellent sensing sensitivity with a gauge factor of 2.78, conductivity of 2.2 S/m, tensile deformation of 200%, fast response time of 370 ms, and recovery time of 260 ms, surpassing those of most previously reported hydrogel-based strain sensors. This improvement can be attributed to the high electrical conductivity and uniform distribution of the rGO associated with Gly and PDA. PGPHs also exhibited an attractive monitoring effect for hand movements and precise detection feedback for the slight dynamics of the pharynx. Hydrogel-based strain sensors have been demonstrated as a potentially sustainable solution for dynamic detection and communication.

Keywords: Composite hydrogels, reduced graphene oxide, strain sensors, dynamic detection

INTRODUCTION

With the development of science and technology, wearable and flexible sensors with skin-friendly properties have attracted the attention of researchers in several fields, such as electronic skin, human-computer interaction, and physiological health detection[1-3]. To achieve the application of soft sensors, it is important for the sensor to possess a high conductivity, which ensures the transmission of electrical signals. The ability of the sensor to transmit signals rapidly and steadily enables the sensitivity and stability of signal acquisition. The excellent mechanical flexibility improves the adaptation to a variety of detection bodies, and the high mechanical tensile properties are beneficial for expanding the range of detection. In addition, biocompatibility is required for personalized monitoring[4,5].

To overcome the inherent stiffness and shape of sensors, 3D printing technology offers an alternative strategy for the preparation of multifunctional electronic devices. The circuit-sensitive elements of the sensor can be constructed on a wide range of flexible substrates, such as fabric, paper, and polymer films. However, the microchannels formed by direct ink writing usually require high-precision processes, making the corresponding 3D printing technology more complex[6-8]. Hydrogels possess excellent mechanical flexibility, stretchability, and biocompatibility. Compared to the traditional sensors made of rigid materials, the hydrogel-based sensors could actively adapt to the surface shape of the tested object. Their preparation process is simple and inexpensive. Therefore, they are promising candidates for wearable sensors.

Due to its low conductivity, the conversion from mechanical to electrical signals in the hydrogel was limited. Researchers have made efforts to solve these issues, such as using conductive polymer materials[9], adding biocompatible materials with high electrical conductivity, including graphene[10], MXene[11,12], and carbon nanotubes[13,14], and adding ions to the hydrogel[15,16]. Lin *et al.* presented a flexible and wearable sensor based on carboxylic styrene-butadiene rubber and hydrophilic sericin noncovalently modified carbon nanotubes with high sensitivity [gauge factor (GF) = 25.98] but low electrical conductivity (0.071 S/m)[13]. To incorporate polyelectrolyte materials, Fan *et al.* introduced carrageenan into polyacrylamide to prepare a double network hydrogel. The addition of NaCl and KCl conferred excellent electrical conductivity and strain sensitivity to the hydrogel, with a conductivity of up to 0.0376 S/cm, and the GF in the linear region (0%-100%) could constantly maintain at 1.956[17]. These reported hydrogel-based strain sensors have not yet achieved a good balance between conductivity and sensitivity. Since the conductivity of hydrogels is provided by ion migration and electron mobility, the general strategy to improve the conductivity is to increase the proportion of conductive media or finely construct a conductive network. If the hydrogel is too dense, the sensitivity will be significantly reduced, resulting in a sluggish response. The adjustment of sensitivity requires comprehensive coordination of the structure and composition of the hydrogel.

Polydopamine (PDA) is skin-friendly and is usually used to improve the biocompatibility of hydrogels. The excellent adhesion ability of PDA is attributed to the presence of several functional groups, such as phenolic hydroxyl and amine groups. The functional groups can not only be used as chemical reaction points for covalent modification of the hydrogel skeleton but also improve the cross-linking interactions between the dopant and backbone material[18-20]. Zhang *et al.* developed a hydrogel composed of PDA-modified reduced graphene oxide (PDA-rGO) nanosheets with polyvinyl alcohol (PVA). The resulting hydrogel exhibited excellent biocompatibility[10]. However, a large number of nanosheets may lead to an uneven internal distribution during the gelation process, causing a reduction in the sensitivity or even instability of the hydrogel-based sensors. Thus, it is challenging to maintain a stable and homogeneous dispersion of graphene or nanosheets in hydrogels.

In this work, we designed conductive hydrogels (PGPHs) comprising rGO, PDA, PVA, and glycerol (Gly) for wearable strain sensors. PVA and rGO are used as the main skeleton and conductive medium, respectively. PDA is used as a carrier for rGO loading and provides hydrogels with excellent skin-friendly properties[18]. Gly assists the rGO prepared by the improved Hummers' method[21] to be uniformly dispersed in an aqueous solution and sequentially forms a homogeneous and stable hydrogel. Figure 1 shows the synthesis principle of PGPHs and their sensing applications. It is found that the PGPHs have high conductivity, excellent sensitivity, reliability, and cycling stability as wearable and flexible strain sensors. This strategy will provide a new avenue for the development of body sensors and accelerate their practical application in this field.

RESULTS AND DISCUSSION

Raman spectroscopy was performed on the as-synthesized graphene oxide (GO) and rGO. The D peak at 1350 cm^{-1} in graphene was primarily caused by the disorderly vibration of graphene, indicating the degree of defects in graphene, whereas the G peak at 1580 cm^{-1} was primarily caused by the vibration of the skeleton sp^2 carbon atoms in graphene [Figure 2A]. The degree of graphene reduction can be derived from the ratio I_D/I_G. When the I_D/I_G ratio of graphene is less than 1, it can be assumed that the main component is GO[22-23]. The X-ray diffraction (XRD) spectra [Figure 2B] of GO and rGO showed that GO had a strong diffraction peak at approximately 10. When rGO was reduced to rGO, the diffraction peak at 10 disappeared and appeared at approximately 23 with a weak and broad peak intensity[23]. From the Raman and XRD spectra of the materials, it can be concluded that the rGO prepared by the reduction of GO exhibited a better response.

Meanwhile, Fourier transform infrared spectroscopy (FTIR) was performed for each component in the experiment to investigate the functional groups in the hydrogel. [Figure 2C and D], the C=O stretching vibration (1,710 cm^{-1}), C=C group resonance (1,570 cm^{-1}), and epoxy C-O (1,228 cm^{-1}) were observed in the FTIR spectrum of rGO[21]. For rGO-PDA, in addition to a more intensive C-N (1,047 cm^{-1}) vibration originating from PDA, numerous O-H vibrations and a strong absorption peak at 3436 cm^{-1} were observed. The FTIR spectrum of PVA hydrogel shows the O-H (3,436 cm^{-1}), C=C (1,630 cm^{-1}), O-H (1,430 cm^{-1}), and C-O (1,090 cm^{-1}) characteristic peaks. After rGO-PDA was added to the gel, the epoxy C-O (1,228 cm^{-1}) on rGO and the C-N (1,047 cm^{-1}) of the PDA absorption peaks became weak, indicating that rGO and PDA were wrapped by PVA[24].

The microstructures of the materials were characterized using scanning electron microscopy (SEM). Figure 3A shows the morphology of GO prepared by Hummers' method as micron-sized flakes. In comparison, the rGO nanosheets [Figure 3B] are smaller. Many rGO nanosheets were stacked during lyophilization, making the surface appear scale-like. As shown in Figure 3C, the rGO/PDA composite formed a structure with a 3D skeleton, and the surface had a scale-like composition of rGO flakes. In contrast, the internal structure of the pure PVA sample exhibited a smooth surface [Figure 3D]. As shown in Figure 3E, PDA particles were observed in the internal structure of the PVA backbone. For the rGO/PDA-PVA sample [Figure 3F], a large amount of scaly lamellar material was observed in the internal structure of the sample, and the pores of the overall structure became smaller, indicating that rGO was attached to the PVA backbone[13,25,26].

The cross-linking of the skeleton network in the hydrogel exhibits a certain randomness and thus might lead to an inhomogeneous connection in the internal structure of the hydrogel, which affects the mechanical properties of the hydrogel. To address this issue, the hydrogel used in this study was produced using a combination of physical and chemical cross-linking. The activation of the carbonyl structure on

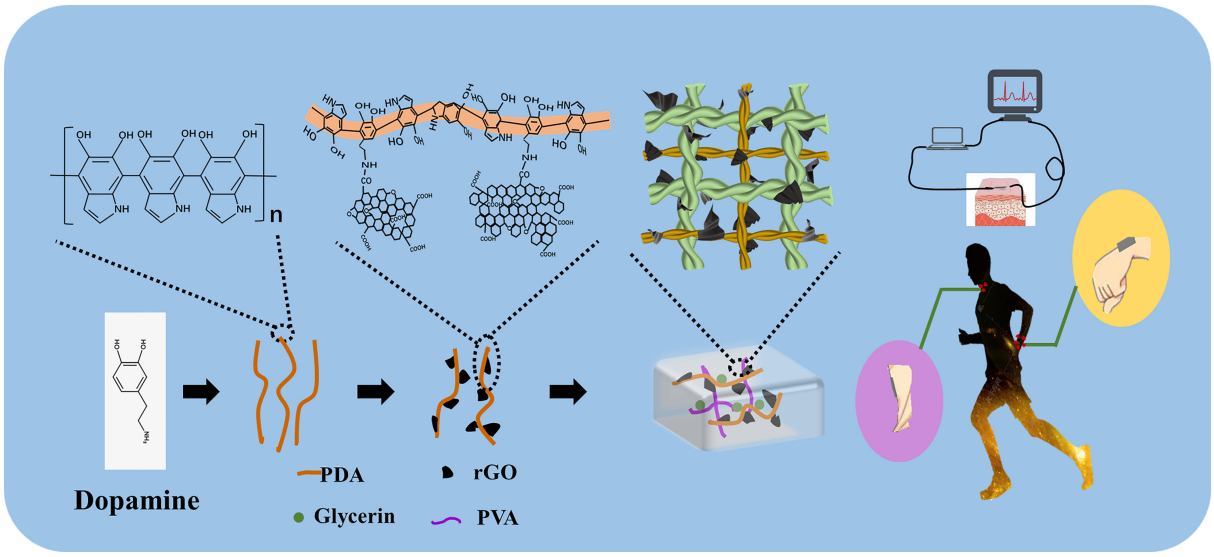

Figure 1. Schematic diagram of the rGO/PDA-Gly-PVA hydrogel synthesis principle and the sensing application. PDA: polydopamine; PVA: polyvinyl alcohol; rGO: reduced graphene oxide.

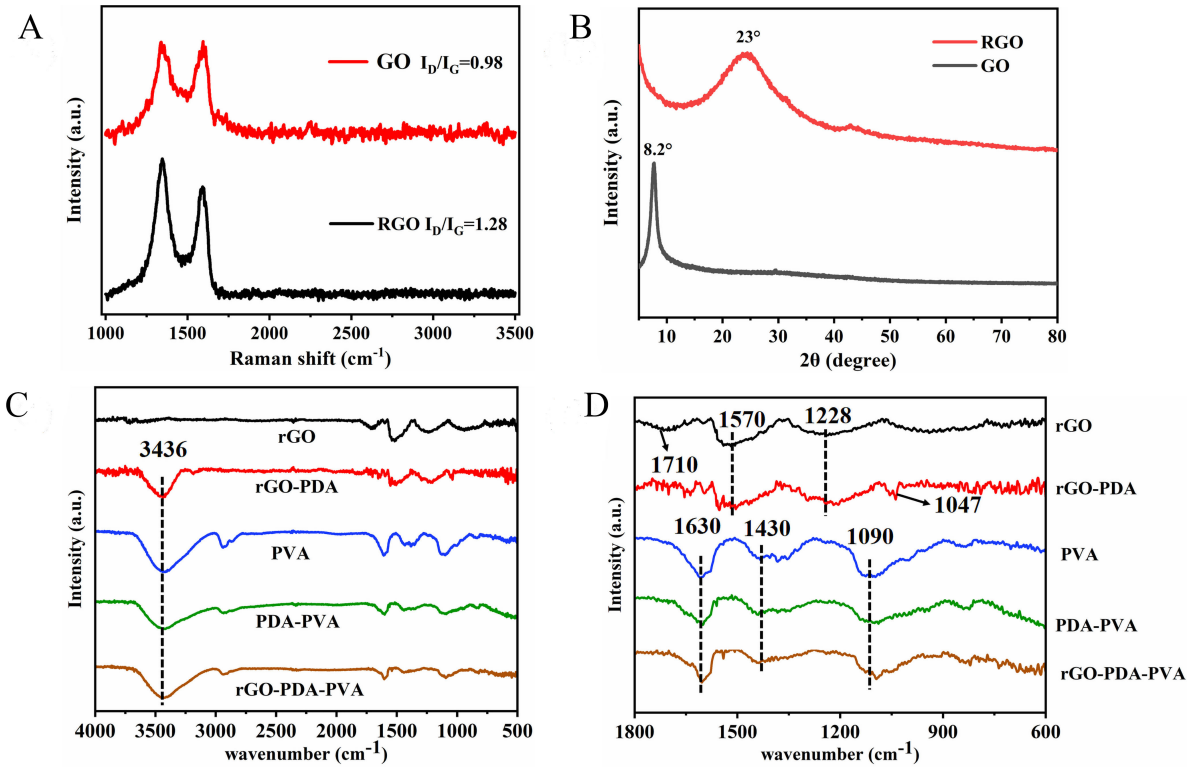

Figure 2. (A) Raman and (B) XRD spectra of GO and rGO; FTIR spectra of different component materials and hydrogels (C) regions within 4,000-500 cm^{-1} and (D) regions within 1,800-600 cm^{-1}. FTIR: fourier transform infrared spectroscopy; rGO: reduced graphene oxide; XRD: X-ray diffraction.

glutaraldehyde (GA) by H^+ catalysis renders the carbonyl atom more active, and the carbonyl structure on the aldehyde dissociates α-H under the induction of protonated O atoms, simultaneously forming an enol structure[27,28]. Relying on GA as the cross-linking agent, a hydroxyl aldehyde condensation reaction occurs

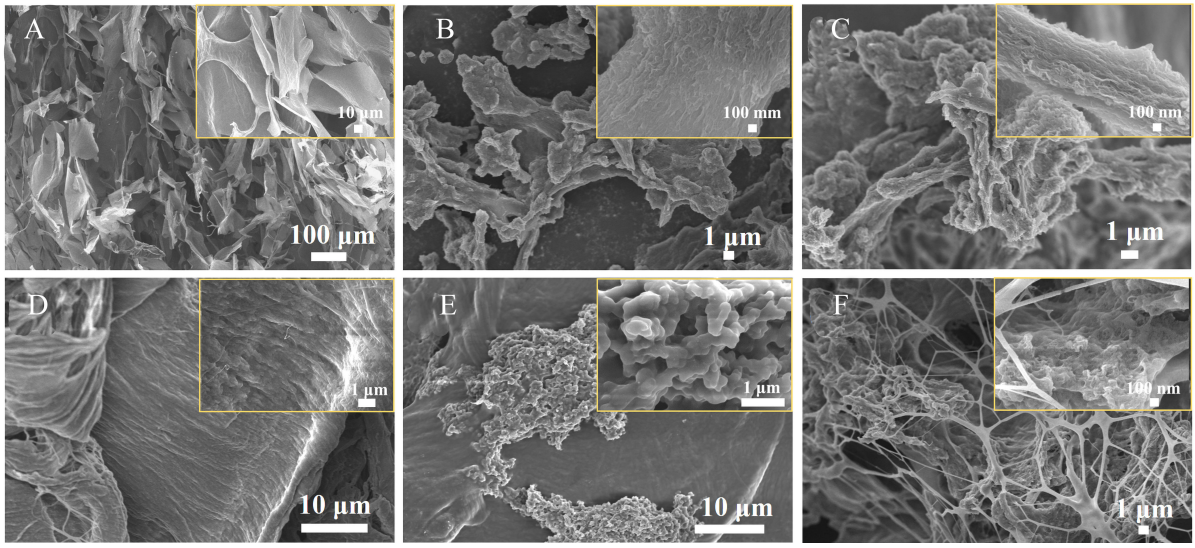

Figure 3. SEM results of freeze-dried materials and hydrogels (A) GO; (B) rGO; (C) rGO/PDA; (D) pure PVA; (E) PDA-PVA; and (F) rGO/PDA-Gly-PVA. Gly: glycerol; PDA: polydopamine; PVA: polyvinyl alcohol; rGO: reduced graphene oxide; SEM: scanning electron microscopy.

to establish the first layer of the network structure via chemical cross-linking[10]. The hydroxyl groups (-OH) of PVA are more abundant than the aldehyde groups (-CHO) of GA, and thus the crosslinker is completely consumed during the reaction process[29-33]. Second, the hydrogel is rapidly cryogenically frozen, which is similar to the traditional freeze-thaw method of PVA hydrogel preparation. The frozen molecular chains of PVA are close to or in contact with each other, resulting in chain entanglement due to van der Waals forces and hydrogen bonding. When the hydrogel was thawed, the molecular chains regained their flow state. When the hydrogel is frozen again, it produces more entangled nodes, thus improving its mechanical properties. Hydrogels exhibit good mechanical properties owing to the double-layer network effect of chemical and physical cross-linking. In this study, the effects of the PVA and PDA contents on the mechanical properties of different hydrogels were investigated.

The mechanical properties of the hydrogels were further investigated to verify the effects of PVA. The barbell-shaped samples for mechanical property tests were prepared in the standard mold [Supplementary Figures 1 and 2]. The hydrogel (with a length of 5 cm) can be easily stretched to more than 12 cm without being broken and even tied into knots [Supplementary Figure 3]. As displayed in the stress-strain curves of the hydrogel in Figure 4A, the mechanical properties of hydrogels with 1wt%-2wt% PVA were poor, and the elongation at break is only 175%-180%. As the PVA content increased, the tensile deformation of the hydrogels gradually increased. When the PVA was 3wt%, the tensile strain of the hydrogel increased to a peak value of 235%. As the PVA content in the hydrogel increased, the tensile strength of the gel gradually increased from 16 kPa to 19 kPa, indicating that the cross-linked structure of the hydrogel gradually tightened. Simultaneously, as the degree of cross-linking of the hydrogel structure increased, its flexibility decreased. As shown in Figure 4B, when the PVA content is 1wt%-2wt%, the sample has good flexibility and can fit the copper sheet with a small bending radius, whereas with an increase in the content, the radius of the sample fitting to the bending copper sheet increases. The flexibility was very poor when the hydrogel with the 5wt% PVA was bent. Since both moderate tensile properties and flexibility are necessary for the hydrogel-based strain sensors, the hydrogel with 2wt% PVA can satisfy the requirement.

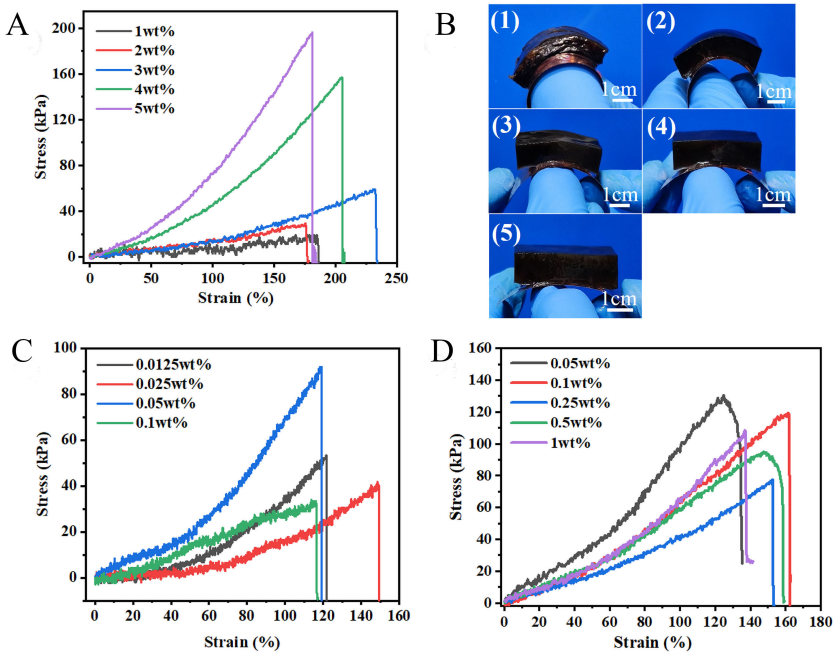

Figure 4. (A) Stress-strain curves and (B) optical images of the hydrogel in the bending states corresponding to different PVA contents; stress-strain curves corresponding to different contents of (C) PDA and (D) rGO in the samples. PDA: polydopamine; PVA: polyvinyl alcohol; rGO: reduced graphene oxide.

The addition of PDA made the hydrogel more flexible; however, excess PDA decreased the strain and flexibility of the hydrogel. As shown in Figure 4C, the effect of PDA content on the tensile deformation performance of the hydrogel first enhanced the deformation and then decreased. When the content was 0.025wt%, the sample exhibited a higher tensile strength with 148% elongation at break. The addition of graphene nanosheets can improve the degree of cross-linking between the skeletal scaffolds [Figure 4D]. However, because the ratio of rGO addition is very small for the entire hydrogel material, it has almost no effect on the mechanical properties of the hydrogel.

Electrical conductivity is an important sensor property. Figure 5A shows the conductivity corresponding to the change in the mass fraction of PVA in the PGPHs. PVA is a polymer with poor conductivity; therefore, the conductivity of the hydrogel gradually decreased as the percentage of PVA in the hydrogel increased. The conductivity of PGPHs was approximately 2.25 S/m when the mass fraction of PVA during 1wt%-2wt%. However, it rapidly dehydrated after approximately 24 h when the amount of PVA in the hydrogel exceeded 2wt%. If the PVA content is too low, it is insufficient to establish a skeletal structure alone. As the main skeleton of the tissue, PVA contains numerous hydroxyl groups that can form hydrogen bonds with water molecules in the hydrogel. Although the skeletal structure of PGPHs was stable and water retention capacity was improved by Gly, the conductivity was considerably reduced with increasing PVA content. Therefore, PGPHs prepared with 2wt%-3wt% PVA can achieve a good balance between structural stability and conductivity.

As the main conductive medium, rGO possesses a carbon-ring structure. The solution formed by ultrasonic dissolution in water is unstable, and rGO easily precipitates with weak hydrophilicity. rGO could not be dispersed uniformly in the hydrogel and was deposited at the bottom as the gel was formed. The colors of the frontage, internal side, and side views were different from the reverse side of the hydrogel, whereas the

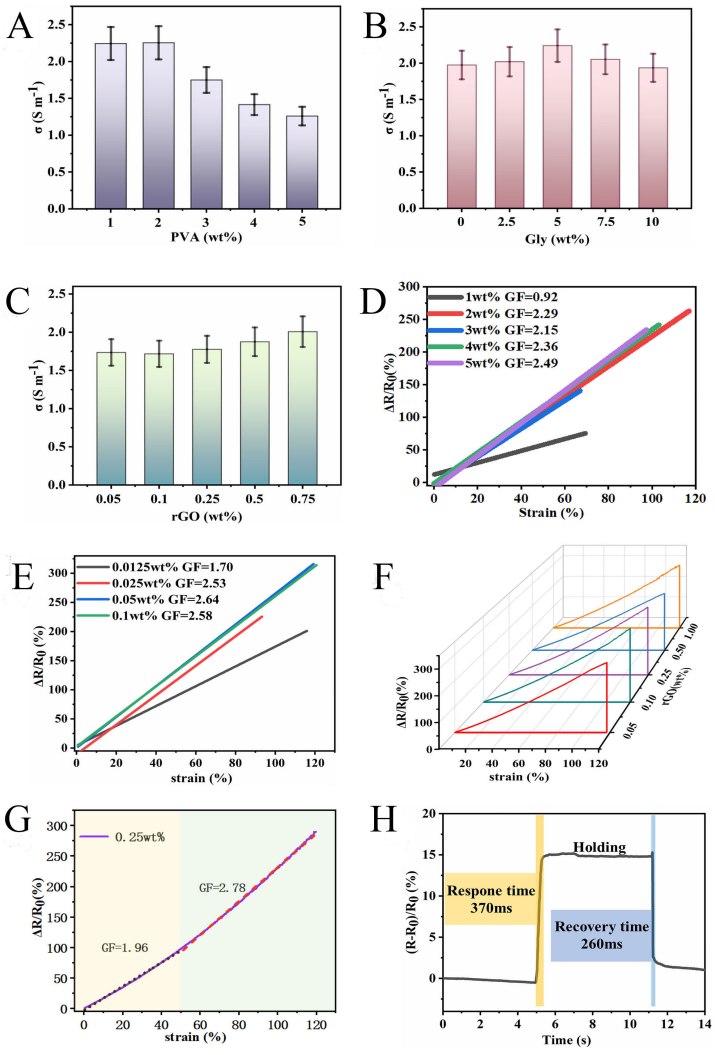

Figure 5. Conductivity of hydrogel with different contents of (A) PVA, (B) Gly, and (C) rGO; Sensitivity of hydrogel based on different contents of (D) PVA, (E) PDA, and (F) rGO; (G) Sensitivity of hydrogel samples with 0.25 wt% rGO content at different deformation rates; (H) Response time and recovery time of hydrogel as a sensor test. Gly: glycerol; PDA: polydopamine; PVA: polyvinyl alcohol; rGO: reduced graphene oxide.

hydrogel with Gly was uniform. This indicated that the addition of Gly caused graphene to be uniformly dispersed in the hydrogel [Supplementary Figure 4]. Gly was added as an auxiliary agent to the rGO dispersion in the solution because it contains hydroxyl groups. As shown in Supplementary Figure 5, the solutions with and without Gly exhibited different states after standing for one week in the air at room temperature. The solution containing Gly was more uniform and stable than the other solutions. In addition, Gly improved the water retention performance of the hydrogel with a reduced rate of water loss [Supplementary Figure 6]. Figure 5B shows that the conductivity of the hydrogel gradually improved with the addition of Gly. However, excessive Gly also reduces the conductivity because it blocks the rGO from each other, causing electron transport to become slow. Thus, a mass fraction of 5wt% can ensure a conductivity of 2.242 S/m while improving the performance of the dispersed rGO.

The unsaturated structure of the carbon rings endows rGO with a large number of interlaced electron clouds, leading to excellent electrical conductivity for PGPHs. The conductivity of the hydrogel with rGO reaches up to 1.95 S/m, which is much higher than that of rGO-free hydrogel [Supplementary Figure 7]. As shown in Figure 5C, the electrical conductivity of the PGPHs also increased with increasing rGO content. The conductivity was higher at 0.75 wt%, reaching more than 2 S/m.

For PGPHs as strain sensors, sensitivity is another key point. As shown in Figure 5D, the sensitivity increased with the proportion of PVA in PGPHs. When the PVA content was more than 2wt%, the GF of the PGPHs was more than 2, indicating that the PGPHs possess high sensitivity. PDA contains numerous amino groups and generates an interaction force with the hydroxyl groups, which makes the structure more stable. The catechol and amine functional groups of PDA have strong binding affinities for a wide range of nanomaterials. PDA can be covalently anchored to oxygen-containing functional groups on rGO nanosheets via Schiff base or Michael addition reactions. The amine group of PDA also aids the growth of rGO through interactions with a large number of carboxyl groups[32-33]. The simultaneous action of various bonds helps PGPHs stabilize their skeletons. The effect of the PDA content on the sensitivity of the PGPHs is shown in Figure 5E. When the PDA content was 0.0125wt%, the GF content was 1.7. As the PDA content increased, the GF content also increased. After reaching 0.05wt%, the GF no longer increased, indicating that the further increase of PDA might not contribute to the GF of PGPHs. The curves in Figure 5F, corresponding to the deformation-relative resistance changes of PGPHs with different rGO contents, almost overlapped. However, after 50% deformation, the slope of the curve significantly increased, and a curve fitting the 0.025 wt% content was obtained [Figure 5G]. When the tensile deformation of the PGPHs was 0-50%, the GF was 1.96. While in 50%-120% of the tensile deformation, the GF could reach up to 2.78. These results show that PGPHs have promising prospects for application as sensors with high conductivity and outstanding sensitivity by regulating the proportion of components. In addition, the response time of the PGPHs as a sensor to the action was 370 ms, and the recovery time was 260 ms [Figure 5H].

Several main parameters of the PGPHs were compared with those of other reported strain sensors [Figure 6A]. It is difficult for most conductive hydrogels to achieve excellent conductivity and sensing sensitivity. Compared to other strain sensors, the sensor prepared herein guarantees overall electrical conductivity without sacrificing high sensitivity.

Stability is important under fluctuations in tensile deformation, testing speed, and stretching periods[32,34,35]. Figure 6B and C shows the stability of PGPH-1 (0.0125wt% rGO-0.025wt% PDA-2wt% PVA) at 10 mm/min testing speed and 50%/min strain rate. The values of $\Delta R/R_0$ can be recovered quickly and maintained at the same level after several cycles of PGPH-1 under both low and high tensile deformations. The $\Delta R/R_0$ was consistent at different testing speeds under 60% deformation [Figure 6D]. The intensity of the $\Delta R/R_0$ peak of the hydrogel was the same for several scanning cycles at the same tensile deformation and scanning rate. However, as the scanning time increased, the resistance increased because of the water loss inside the hydrogel [Figure 6E].

The use of PGPHs as strain sensors has been demonstrated by the dynamic detection of different human body parts based on their stability, reliability, and detection specificity[36-37] When the hydrogel is stretched or, in the case of other stimuli, the output resistance is reduced because the intertwined and staggered electron clouds shorten the electron transport path. When the action returned to the initial rotational state, the resistance also returned to the initial rotational state. The peak resistance change is an order of magnitude owing to the difference in the strength of each movement, although the shape remains unchanged. Figure 7A-C shows the dynamic detection of the slight movements of the sensor on the human

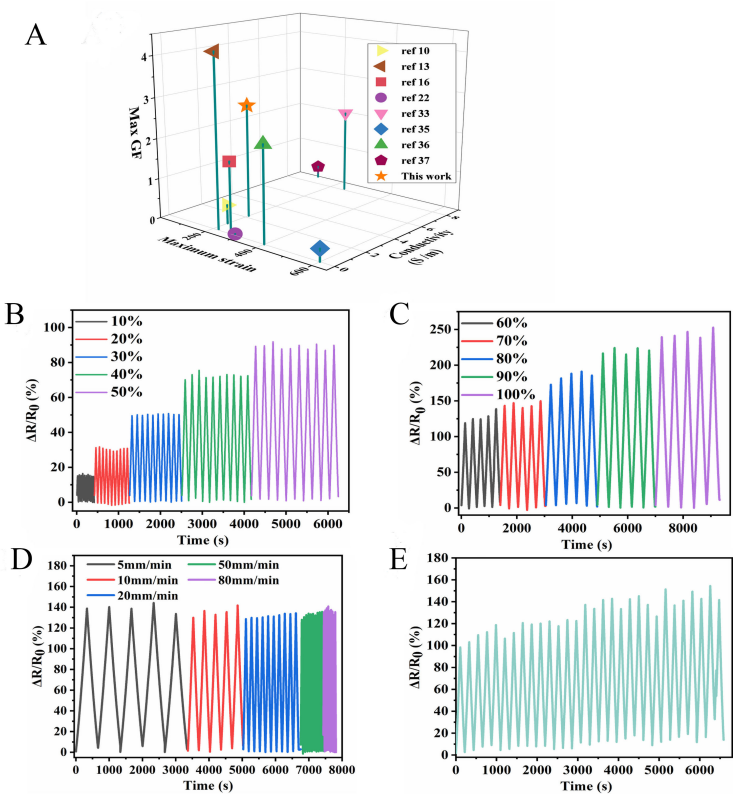

Figure 6. (A) Performance comparison with other conductive hydrogel-based sensors; resistance response of the sensor under (b) low and (c) high tensile deformation (10 mm/min testing speed, 50%/min strain rate); (D) resistance response of the sensor at different testing speeds under 60% strain; (E) durability test of the sensor (10 mm/min testing speed, 50%/min strain rate, and 60% strain).

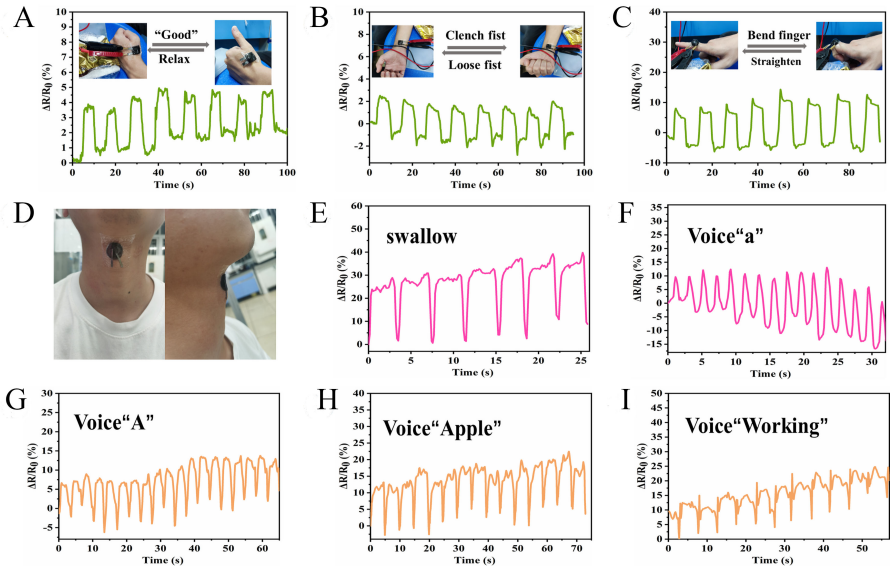

Figure 7. Performance of hydrogel as a sensor in physiological detection (A) the detection point is the masseter muscle, the thumb makes a "GOOD" gesture; (B) the detection point is the wrist, the hand makes a fist and slightly raises; (C) the detection point is the index finger joint, the finger is straightened to bent; (D) the detection point of hydrogel is the human throat; (E) the pharynx makes a swallowing motion; (F) vocalizing "a" [a:]; (G) vocalizing "A" "[ei]"; (H) vocalizing "Apple"; (I) vocalizing "Working".

body, and the detection curves of the three parts were specific and repeatable. Figure 7A shows the real-time relative resistance performance of the sensors during the dynamic process of lifting and lowering the masseter muscle. The detection performance of the muscle at the inner wrist as the hand switched between the clenched and relaxed states and the monitoring of the bending recovery of the index finger are shown in Figure 7B and C, respectively. Figure 7D shows a photograph of the sensor used to detect the pharyngeal signals. The detection performance of the sensor when the human pharynx is swallowed or vocalized with a slight vibration of the vocal folds is shown in Figure 7E-I. The waveform had a sharp single peak when the pronunciation was just one syllable. In contrast, the waveform showed two small adjacent peaks if the pronunciation had two syllables. Therefore, this study can help groups that cannot be vocalized because of acquired encounters. The sensor can transform vocalizations into specific waveforms that can be recognized and transformed into relevant words.

CONCLUSIONS

In summary, the PGPHs with excellent conductivity (more than 2.2 S/m) and sensitivity (GF of up to 2.78) have been successfully prepared, and the addition of PDA endowed the hydrogel with good biocompatibility. The designed composite organohydrogel was assembled as a signal acquisition and sensing component for wearable strain sensors. The sensor rapidly responded (370 ms) and recovered (260 ms). It possesses highly sensitive signal acquisition capability and transmission stability when detecting minor human movement behaviors or weak signals, such as wrist and hand movements, throat swallowing movements, and vocal cord vibrations during vocalizations. The composite hydrogel has the potential to be used as a wearable strain sensor for human-computer interactions and medical applications. This sensor is also expected to be used in the future to help groups of people whose vocal cords vibrate but who are unable to communicate verbally. Although hydrogel-based sensors are currently limited to the reciprocal translation of signals, they will drive the rapid development of the personalized medicine, human-computer interaction, and intelligent robots.

DECLARATIONS

Authors' contributions

Data curation, formal analysis, investigation, methodology, writing original draft: Ke X
Interpreting the data: Mu X, Chen S, Zhang Z, Chen Y
Drafting this work and revising it critically for main intellectual content: Zhou J, Gao J, Liu J, Wang X, Ma C, Miao L

Availability of data and materials

Not applicable.

Financial support and sponsorship

This work was supported by the Scientific Research and Technology Development Program of Guangxi (No. ZY21195037). Natural Science Foundation of Guangxi Province (No. 2019GXNSFFA245010). National Natural Science Foundation of China (No. 52173094 and 52003062).

Conflicts of interest

All authors declared that there are no conflicts of interest.

Ethical approval and consent to participate

Not applicable.

Consent for publication

Not applicable.

REFERENCES

1. Li S, Pan H, Wang Y, Sun J. Polyelectrolyte complex-based self-healing, fatigue-resistant and anti-freezing hydrogels as highly sensitive ionic skins. *J Mater Chem A* 2020;8:3667-75. DOI
2. Baumgartner M, Hartmann F, Drack M, et al. Resilient yet entirely degradable gelatin-based biogels for soft robots and electronics. *Nat Mater* 2020;19:1102-9. DOI
3. Lei Z, Wu P. A supramolecular biomimetic skin combining a wide spectrum of mechanical properties and multiple sensory capabilities. *Nat Commun* 2018;9:1134. DOI PubMed PMC
4. Feng Y, Liu H, Zhu W, et al. Muscle-inspired mxene conductive hydrogels with anisotropy and low-temperature tolerance for wearable flexible sensors and arrays. *Adv Funct Materials* 2021;31:2105264. DOI
5. Huang J, Wang H, Li J, et al. High-performance flexible capacitive proximity and pressure sensors with spiral electrodes for continuous human-machine interaction. *ACS Materials Lett* 2022;4:2261-72. DOI
6. Goh GL, Zhang H, Chong TH, Yeong WY. 3D printing of multilayered and multimaterial electronics: a review. *Adv Electron Mater* 2021;7:2100445. DOI
7. Oh J, Bae J. A direct ink writing based fabric-embedded soft sensor for improved durability and sewability. *Smart Mater Struct* 2022;31:065020. DOI
8. Kim S, Oh J, Jeong D, Park W, Bae J. Consistent and reproducible direct ink writing of eutectic gallium-indium for high-quality soft sensors. *Soft Robot* 2018;5:601-12. DOI PubMed
9. Javadi M, Gu Q, Naficy S, et al. Conductive tough hydrogel for bioapplications. *Macromol Biosci* 2018;18:1700270. DOI
10. Zhang H, Ren P, Yang F, et al. Biomimetic epidermal sensors assembled from polydopamine-modified reduced graphene oxide/polyvinyl alcohol hydrogels for the real-time monitoring of human motions. *J Mater Chem B* 2020;8:10549-58. DOI
11. Li X, He L, Li Y, et al. Healable, degradable, and conductive mxene nanocomposite hydrogel for multifunctional epidermal sensors. *ACS Nano* 2021;15:7765-73. DOI
12. Guo J, Yu Y, Zhang D, Zhang H, Zhao Y. Morphological hydrogel microfibers with mxene encapsulation for electronic Skin. *Research* 2021;2021:7065907. DOI PubMed PMC
13. Lin M, Zheng Z, Yang L, et al. A high-performance, sensitive, wearable multifunctional sensor based on rubber/CNT for human motion and skin temperature detection. *Adv Mater* 2022;34:e2107309. DOI PubMed
14. Yu J, Feng Y, Sun D, Ren W, Shao C, Sun R. Highly conductive and mechanically robust cellulose nanocomposite hydrogels with antifreezing and antidehydration performances for flexible humidity sensors. *ACS Appl Mater Interfaces* 2022;14:10886-97. DOI
15. Liang D, Zhou G, Hu Y, Zhao C, Chen C. Metal cation-ligand interaction modulated mono-network ionic conductive hydrogel for wearable strain sensor. *J Mater Sci* 2021;56:14531-41. DOI
16. Hu J, Wu Y, Yang Q, et al. One-pot freezing-thawing preparation of cellulose nanofibrils reinforced polyvinyl alcohol based ionic hydrogel strain sensor for human motion monitoring. *Carbohydr Polym* 2022;275:118697. DOI
17. Fan Z, Duan L, Gao G. Self-healing carrageenan-driven polyacrylamide hydrogels for strain sensing. *Sci China Technol Sci* 2020;63:2677-86. DOI
18. Yang L, Wang Z, Fei G, Xia H. Polydopamine particles reinforced poly(vinyl alcohol) hydrogel with NIR light triggered shape memory and self-healing capability. *Macromol Rapid Commun* 2017;38:1700421. DOI
19. Zhao Y, Li Z, Song S, et al. Skin-inspired antibacterial conductive hydrogels for epidermal sensors and diabetic foot wound dressings. *Adv Funct Mater* 2019;29:1901474. DOI
20. Panwar V, Babu A, Sharma A, et al. Tunable, conductive, self-healing, adhesive and injectable hydrogels for bioelectronics and tissue regeneration applications. *J Mater Chem B* 2021;9:6260-70. DOI
21. Zhou J, Gu Y, Deng Z, et al. The dispersion of Au nanorods decorated on graphene oxide nanosheets for solar steam generation. *SM&T* 2019;19:e00090. DOI
22. Jing X, Mi H, Napiwocki BN, Peng X, Turng L. Mussel-inspired electroactive chitosan/graphene oxide composite hydrogel with rapid self-healing and recovery behavior for tissue engineering. *Carbon* 2017;125:557-70. DOI
23. Yang J, Yu W, Zhang Y, Liu C, Xie H. Graphene double cross-linked thermally conductive hydrogel with low thermal contact resistance, flexibility and self-healing performance. *Int Commun Heat Mass Trans* 2021;127:105537. DOI
24. Han L, Zhang Y, Lu X, Wang K, Wang Z, Zhang H. Polydopamine nanoparticles modulating stimuli-responsive PNIPAM hydrogels with cell/tissue adhesiveness. *ACS Appl Mater Interfaces* 2016;8:29088-100. DOI
25. Yin J, Liu Q, Zhou J, et al. Self-assembled functional components-doped conductive polypyrrole composite hydrogels with enhanced electrochemical performances. *RSC Adv* 2020;10:10546-51. DOI PubMed PMC
26. Li C. Towards conductive hydrogels in e-skins: a review on rational design and recent developments. *RSC Adv* 2021;11:33835-48.

DOI PubMed PMC

27. Zhao D, Liao G, Gao G, Liu F. Influences of intramolecular cyclization on structure and cross-linking reaction processes of PVA hydrogels. *Macromolecules* 2006;39:1160-4. DOI
28. Luo D, Guo L, Wang Y, Wang P, Chang Z. Novel synthesis of PVA/GA hydrogel microspheres based on microfluidic technology. *J Flow Chem* 2020;10:551-62. DOI
29. Tanpichai S, Oksman K. Cross-linked nanocomposite hydrogels based on cellulose nanocrystals and PVA: Mechanical properties and creep recovery. *Compos Part A Appl Sci Manuf* 2016;88:226-33. DOI
30. Fan L, Mei X, Zhang J, et al. Effect of multi-walled carbon nanotube on thermal decomposition, mechanical and heat-induced shape memory properties of crosslinked poly(vinyl alcohol). *Smart Mater Struct* 2021;30:115017. DOI
31. Sun X, Fujimoto T, Uyama H. Fabrication of a poly(vinyl alcohol) monolith via thermally impacted non-solvent-induced phase separation. *Polym J* 2013;45:1101-6. DOI
32. Jing X, Mi H, Peng X, Turng L. Biocompatible, self-healing, highly stretchable polyacrylic acid/reduced graphene oxide nanocomposite hydrogel sensors via mussel-inspired chemistry. *Carbon* 2018;136:63-72. DOI
33. Xie Z, Li H, Mi H, Feng P, Liu Y, Jing X. Freezing-tolerant, widely detectable and ultra-sensitive composite organohydrogel for multiple sensing applications. *J Mater Chem C* 2021;9:10127-37. DOI
34. Ge G, Lu Y, Qu X, et al. Muscle-Inspired self-healing hydrogels for strain and temperature sensor. *ACS Nano* 2020;14:218-28. DOI
35. Guo Y, Zhou X, Tang Q, Bao H, Wang G, Saha P. A self-healable and easily recyclable supramolecular hydrogel electrolyte for flexible supercapacitors. *J Mater Chem A* 2016;4:8769-76. DOI
36. Zhao R, Jiang L, Zhang P, Li D, Guo Z, Hu L. Graphene oxide-based composite organohydrogels with high strength and low temperature resistance for strain sensors. *Soft Matter* 2022;18:1201-8. DOI
37. Sun X, Yao F, Wang C, et al. Ionically conductive hydrogel with fast self-recovery and low residual strain as strain and pressure sensors. *Macromol Rapid Commun* 2020;41:e2000185. DOI PubMed